**Palbociclib has anti-tumoral effects on PTEN deficient endometrial neoplasias**

Maria Alba Dosil[1,2], Cristina Mirantes[1], Núria Eritja[1,2], Isidre Felip[1], Raúl Navaridas[1], Sònia Gatius[1,2], Maria Santacana[1,2], Eva Colàs[3], Cristian Moiola[3], Joan Antoni Schoenenberger[4], Mario Encinas[5], Eloi Garí[6*], Xavier Matias-Guiu[1,2*], Xavier Dolcet[1,2*]

[1]Oncologic Pathology Group. Dept. Ciències Mèdiques Bàsiques, Universitat de Lleida. Hospital Universitari Arnau de Vilanova. Institut de Recerca Biomèdica de Lleida, IRBLleida. Lleida, Spain.

[2]Oncologic Pathology Group. Dept. Ciències Mèdiques Bàsiques, Universitat de Lleida. Hospital Universitari Arnau de Vilanova. Institut de Recerca Biomèdica de Lleida, IRBLleida. Lleida, Spain. Centro de Investigación Biomédica en Red de Oncología (CIBERONC), Madrid, Spain.

[3]Biomedical Research Group in Gynecology, Vall Hebron Research Institute (VHIR), Universitat Autònoma de Barcelona, Barcelona, Spain

[4]Dept. of Pharmacology. Hospital Universitari Arnau de Vilanova. Institut de Recerca Biomèdica de Lleida, IRBLleida. Lleida, Spain

[5]Dept. Medicina Experimental, Universitat de Lleida. Institut de Recerca Biomèdica de Lleida, IRBLleida. Lleida, Spain

[6]Cell Cycle Group. Dept. Ciències Mèdiques Bàsiques, Universitat de Lleida. Institut de Recerca Biomèdica de Lleida, IRBLleida. Lleida, Spain

*Senior co-authors

Running title: Inhibition of Cyclin D-CDK4/6 axis in PTEN-deficient neoplasias.

We declare no conflict of interests

Address all correspondence to:

Xavi Dolcet, PhD

Dept. de Ciències Mèdiques Bàsiques

Universitat de Lleida/IRBLleida

Ed Biomedicina I, Hospital Arnau de Vilanova,

Av. Rovira Roure 80

25198 Lleida

Spain

Email: dolcet@cmb.udl.cat

Phone: +34 973 702951

**Abstract**

PTEN is one of the most frequently mutated genes in human cancers. The frequency of PTEN alterations is particularly high in endometrial carcinomas. Loss of PTEN leads to a dysregulation of cell division and promotes the accumulation of cell cycle complexes such as Cyclin D1-CDK4/6, which is an important feature of the tumoral phenotype. Cell cycle proteins have been presented as key targets in the treatment of the pathogenesis of cancer, and several CDK inhibitors have been developed as a strategy to generate new anticancer drugs. Palbociclib (PD-332991) specifically inhibits CDK4/6 and it has been approved for its use in metastatic breast cancer in combination with letrazole. Here, we have used a tamoxifen-inducible PTEN knock-out mouse model to assess the anti-tumoral effects of Cyclin D1 knock-out and CDK4/6 inhibition by Palbociclib on endometrial tumors. Interestingly, both Cyclin D1 deficiency and Palbociclib treatment trigger shrinkage of endometrial neoplasias. In addition, Palbociclib treatment significantly increases PTEN deficient mice survival and, as expected, has a general effect reducing tumor-cell proliferation. To further analyze the effects of Palbociclib on endometrial carcinoma, we have established subcutaneous tumors with human endometrial cancer cell lines and primary endometrial cancer xenografts, which allow us to provide more translational and predictive data. To date, this is the first pre-clinical study evaluating the response to CDK4/6 inhibition in endometrial malignancies driven by PTEN deficiency, unveiling an important role of the Cyclin D-CDK4/6 activity in their development.

Keywords: PTEN, endometrial carcinoma, Cyclin D1, CDK4/6, Palbociclib

## Introduction

Activation of the phosphatidylinositol 3-kinase/protein kinase B (PI3K/AKT) promotes cell survival and proliferation. The most important negative regulator of this pathway is PTEN (phosphatase and tensin homolog deleted on chromosome 10), which antagonizes the PI3K activity by dephosphorylating phosphatidylinositol (3,4,5)-trisphosphate (PIP3) to phosphatidylinositol (4,5)-bisphosphate (PIP2)[1,2].

PTEN is one of the most frequently mutated genes in human cancers[3]. The frequency of PTEN alterations is particularly high in endometrial carcinomas (EC), which are the most common tumors of the female genital tract[4]. Nearly 70% of endometrial tumors present PTEN alterations[5].

The role of PTEN in carcinogenesis has been validated by different knock-out mouse models[6-8]. Recently, our group has generated a tamoxifen-inducible PTEN knock-out mouse model. Loss of PTEN leads to extremely rapid and efficient development of endometrial hyperplasias and *in situ* carcinomas, prostate neoplasias and thyroid hyperplasias[9].

It is well-known that absence of PTEN triggers an abnormal cell division and alters the expression of cell cycle regulators such as Cyclin D1[9]. The Cyclin D-CDK4/6 signaling axis is important for cell division and tumor growth[10,11]. The D-type Cyclin family is composed by three different proteins (D1, D2 and D3) and its expression is induced upon cell exposure to mitogens. Therefore, D-type Cyclins link cell environment to machinery that drives cell cycle progression[12,13]. Overexpression of the D-type Cyclins and/or CDK4/6 proteins is commonly seen in a number of human tumors. Cyclin D1 is

overexpressed in numerous neoplasms of prostate and endometrium[10,14-16]. In breast cancer, overexpression reaches approximately 50% of the cases[17].

CDK inhibiton has been presented as a strategy to generate new anticancer drugs. The effectiveness of CDK4 and CDK6 inhibition in cancer is being assessed with highly selective inhibitors, such as Palbociclib[10,18,19], which specifically inhibits CDK4/6, but not the other CDKs[20].

Here, we have first studied PTEN-driven tumorigenesis in the context of Cyclin D1 deficiency. Next, we have used a tamoxifen-inducible PTEN knock-out mouse model and different approaches with human endometrial cancer cell lines to assess the anti-tumoral effects of Palbociclib. Finally, we have also performed primary endometrial cancer xenografts to provide more translational research data. Our results demonstrate that Palbociclib treatment triggers shrinkage of endometrial lesions and reduces tumor cell proliferation. To date, this is the first pre-clinical study evaluating the response to Palbociclib in endometrial malignancies driven by PTEN deficiency.

## Materials and methods

### Cell lines and culture conditions

Endometrial carcinoma cell lines were grown in two dimensions and in three-dimensional (3D) cultures as previously described[21,22]

### Cell viability and cell cycle distribution analysis

Cell viability and cell cycle distribution was evaluated as previously described[21,23].

### Isolation of endometrial epithelial cells and establishment of 3D cultures

Isolation of mouse endometrial epithelial cells and establishment of 3D cultures were performed as previously described[24].

When required, PTEN deletion in endometrial cells isolated from Cre:$ER^{T+/-}$-$PTEN^{fl/fl}$ mice was induced by addition of 0.5 µg/ml of tamoxifen in culture medium.

### Bromodeoxyuridine Incorporation

The bromodeoxyuridine protocol was performed as previously described[24].

### Confocal Imaging and Spheroid Diameter Evaluation

Images of endometrial epithelial spheroids were captured and digitized as previously described[25]. Epithelial glands diameter analysis was processed by image analysis software (ImageJ version 1.46r; NIH, Bethesda, MD).

**RNA extraction, Reverse transcriptase-polymerase chain reaction (RT-PCR) and quantitative real-time PCR (RT-qPCR)**

Total RNA was extracted following manufacturer's instructions (RNeasy Total RNA kit; Qiagen, Valencia, CA, USA). RNA was retrotranscribed to cDNA using the High Capacity cDNA Archive Kit (Applied Biosystems, Foster City, USA). The cDNA product was used as a template for subsequent PCR.

Relative mRNA expression levels were calculated using the 2ΔΔCt method and Ct values were normalized to the housekeeping gene β-Glucuronidase (GusB). Taqman® technology from Applied Biosystems was used for real-time RT-qPCR analyses. Probes used are detailed in supplementary table 1 (Supporting Information).

**Animals**

Mice were maintained as previously described[23]. The *in vivo* studies complied with Law 5/1995 and Act 214/1997 of the Autonomous Community (Generalitat de Catalunya) and EU Directive EEC 63/2010, and were approved by the Ethics Committee on Animal Experiments of the University of Lleida and the Ethics Commission in Animal Experimentation of the Generalitat de Catalunya.

Cre:ER$^{T+/-}$ PTEN$^{f/f}$ mice were generated as previously described[9]. Cyclin D1 (referred here as CycD1) knock-out mice were obtained from the Jackson Laboratory (Bar Harbor, ME). Cre:ER$^{T+/-}$ PTEN$^{f/f}$ CycD1$^{-/-}$ mice were bred by crossing Cre:ER$^{T+/-}$ PTEN$^{f/f}$ and CycD1$^{-/-}$ mice (Sup.Fig.1A).

Immunodeficient SCID mice were maintained in Specific Pathogen Free (SPF) conditions.

**Tamoxifen**

Tamoxifen was dissolved and administered as previously described[9].

**Palbociclib**

Palbociclib was obtained from Pfizer Inc. Palbociclib powder was stored at room temperature and protected from light.

For *in vitro* experiments, a 2.5 mM stock of Palbociclib was prepared in DMSO and stored as single use aliquots at -80ºC.

For *in vivo* experiments, Palbociclib was dissolved in Sodium L-Lactate (Sigma-Aldrich; St. Louis, MO) buffer (50mM, pH 4.0). Cre:ER$^{T+/-}$ PTEN$^{f/f}$ mice were given a single daily dose of 100 mg/kg of Palbociclib by oral gavage, starting two weeks after tamoxifen injection. For Palbociclib acute treatment, Cre-ER$^{T+/-}$ PTEN$^{fl/fl}$ animals were treated for three consecutive days with 75, 100 or 150 mg/kg of the inhibitor. For survival experiments, mice received 5 doses per week until the moment of sacrifice. In each experiment, control animals were given vehicle following the same schemes.

**Subcutaneous xenografts and treatment**

Subcutaneous HEC-1A or MFE-296 cells-derived tumors were developed, maintained and measured as previously described[21]. When tumors reached 100 mm$^3$, mice were treated by oral gavage with vehicle or 150 mg/kg Palbociclib for 15 days.

**Patient-derived tumor xenograft (PDX) establishment and treatment**

All animal procedures were performed according to protocols approved by the Animal Experimentation Ethics Committee from the Vall Hebron University Hospital.

A patient-derived tumor xenograft (PDX), PDX741, was generated using fresh primary tumor tissue from an endometrioid endometrial cancer patient by subcutaneously implantation in the animal flanks. For evaluation of drug efficacy, small pieces of PDXs were surgically transplanted subcutaneously into female Swiss nude mice, 6 week old, and allowed to establish. When the tumors reached approximately 200 $mm^3$, mice were randomized into groups of 4-5 mice and treated with vehicle or Palbociclib (150 mg/kg). Mice were treated daily by oral gavage for ten days. Tumors were measured twice weekly with a vernier caliper, and volumes were calculated as $(length \times width^2)/2 = mm^3$.

**Histopathology and Immunohistochemistry**

Histopathological and immunohistochemical studies were performed as previously described[23]. The antibodies used are detailed in supplementary table 2 (Supporting Information).

Immunohistochemical results were graded by considering the intensity of the staining. A histological score was obtained by using an automated imaging system, the ACIS® III Instrument (Dako). An intensity score was obtained from 4 different areas of each sample.

**Proliferation analysis**

Proliferation from Ki-67 and Cyclin D1 immunohistochemistries was calculated as previously described[9].

**Western Blot**

Western Blot was performed as previously described[23]. The antibodies used are detailed in Table 2 (Supporting Information).

**Statistical analysis**

All the experiments were performed at least three times. N indicates the number of mice. Statistical analyses were performed with GraphPad Prism 6.0 software. Values are presented as means ± standard errors of the mean (s.e.m). Data were compared using Student's t-test, one-way ANOVA or two-way ANOVA, with $p < 0.05$ considered as significant. Chi square test was used to compare the incidence of histopathological lesions between groups. Mantel-Cox test, followed by the Gehan-Breslow-Wilcoxon test, was used to compare mice survival between groups.

## Results

### PTEN deletion enhances Cyclin D1 expression.

Previous studies demonstrate that PTEN protein influences Cyclin D1 expression, but the reported results are still controversial[26-28]. To address this issue, we used a tamoxifen-inducible PTEN knock-out mice[9], which rapidly develop endometrial intraepithelial neoplasias (EIN), thyroid hyperplasias and prostatic intraepithelial neoplasias (PIN) between 6-8 weeks after tamoxifen-induced PTEN deletion (Sup.Fig.2A, B and C).

By immunohistochemical analysis, we observed an increment of Cyclin D1 after PTEN loss in endometrium, thyroid and prostate (Sup.Fig.2A, B and C), and this observation was concomitant with Ki-67 increased expression (Sup.Fig.2G). Moreover, Cyclin D1 expression was incremented on lysates from endometrial epithelial 3D cultures, and thyroid or prostate tissues (Sup.Fig.2D, E and F). Collectively, these results indicate that PTEN loss increases Cyclin D1 expression.

### Effects of Cyclin D1 deficiency in PTEN-driven neoplasias.

Having demonstrated that PTEN deficiency correlated with an increment of Cyclin D1, we questioned whether such increase was required to drive PTEN-loss induced tumorigenesis. We generated Cre:$ER^{T+/-}$ $PTEN^{fl/fl}$ $CycD1^{-/-}$ mice to achieve simultaneous loss of PTEN and Cyclin D1 (Sup.Fig.1A). The phenotype of mice lacking Cyclin D1 compromised the viability of Cre:$ER^{T+/-}$ $PTEN^{fl/fl}$ $CycD1^{-/-}$ mice, which limited the number of animals used in the study[29,30].

The experimental workflow is shown in figure 1A and supplementary figures 3A and 4A. Interestingly, Cyclin D1 absence led to a reduction in the incidence and progression of endometrial lesions (Fig.1B). The majority of histological changes found in the endometrium of the Cre:ER$^{T+/-}$ PTEN$^{fl/fl}$ CycD1$^{-/-}$ were classed as hyperplasias, and only a 17% of the animals progressed to EIN, whereas EIN incidence in the wild-type counterparts was near to 53%. Macroscopic analysis revealed no reduction in thyroid (Sup.Fig.3B) and prostate (Sup.Fig.4B) size of Cre:ER$^{T+/-}$ PTEN$^{fl/fl}$ CycD1$^{-/-}$ mice. Furthermore, histological examination revealed that Cyclin D1 deficiency did not impair PTEN tumorigenesis neither in thyroid nor in prostate (Sup.Fig.3C and Sup.Fig.4C).

By Ki-67 immunohistochemistry, we found that endometrium, thyroid and prostate from animals of both genotypes showed the same proliferating rate (Fig.1C, Sup.Fig.3D and Sup.Fig.4D, respectively). Finally, we analyzed the expression of several components of the cell cycle in all three tissues from Cre:ER$^{T+/-}$ PTEN$^{fl/fl}$ CycD1$^{+/+}$ and Cre:ER$^{T+/-}$ PTEN$^{fl/fl}$ CycD1$^{-/-}$ mice. As depicted in figure 1D and supplementary figures 3E and 4E, absence of Cyclin D1 did not modify the expression of any of the elements analyzed.

Finally, we also analyzed the phosphorylation status of Rb as a biomarker of Cyclin D-CDK4/6 activity. The immunohistochemistry against p-Rb (Ser780), which is specifically phosphorylated by CDK4/6, revealed no blockade of the Cyclin D-CDK4/6 axis in the context of Cyclin D1 absence (Fig.1E, Sup.Fig.3F and Sup.Fig.4F). These results strongly support the hypothesis that proliferation of PTEN deficient malignancies is not dependent on Cyclin D1.

**CDK4/6 inhibition triggers an anti-proliferative effect on mouse PTEN deficient endometrial cells *in vitro.***

In an attempt to understand the molecular basis of the Cyclin D1-independent proliferation and cell cycle progression in PTEN deficient tumors, we hypothesized that compensatory expression of other Cyclins may override the loss of Cyclin D1. We determined the levels of all three D-type Cyclins by RT-qPCR from PTEN proficient and PTEN deficient epithelial endometrial 3D cultures. As depicted in supplementary figure 5A, PTEN ablation not only induced an up-regulation of Cyclin D1 mRNA expression, but also of Cyclin D2 and Cyclin D3.

It seems that loss of PTEN enhances the expression of all the D-type Cyclins, making the absence of a single Cyclin D insufficient to impede the Cyclin D-CDK4/6 axis. For that reason, we evaluated the impact of specific CDK4/6 inhibition on cell proliferation to effectively block Cyclin D-CDK4/6 axis. For this purpose, we established endometrial 3D cultures from Cre:$ER^{T+/-}$ $PTEN^{fl/fl}$ mice treated (PTEN KO) or not (PTEN WT) with tamoxifen to induce PTEN excision. 3D cultures were exposed to Palbociclib for 48 hours. Palbociclib treatment resulted in a significant decrease of glandular size (Sup.Fig.5B) and BrdU-incorporating cells (Sup.Fig.5C). All the above results demonstrate that CDK4/6 inhibition by Palbociclib induces a decrease of endometrial cells proliferation *in vitro*.

**Palbociclib treatment reduces PTEN-induced endometrial carcinoma *in vivo.***

Next, we sought to investigate whether the inhibitor was equally effective *in vivo* in our tamoxifen-inducible PTEN knock-out mouse model. The treatment scheme is shown in figure 2A. Histopathological evaluation revealed that Palbociclib treated animals presented

endometrial lesions of significant lesser extent than the untreated ones. Vehicle treated animals displayed EIN (67%) and severe hyperplasia (33%), whereas most animals receiving Palbociclib showed hyperplasia (40%) and severe hyperplasia (40%). Moreover, only 10% of the lesions progressed to EIN, and another 10% conserved normal histology (Fig.2B). In addition, uteri from Cre:ER$^{T+/-}$ PTEN$^{f/f}$ mice treated with the inhibitor presented a substantial reduction of the Ki-67 proliferation marker in comparison with the untreated ones (Fig.2C).

In other tissues, macroscopic analysis revealed a dramatic reduction in thyroid and prostate size and weight (Sup.Fig.6B and Sup.Fig.7B) from Cre:ER$^{T+/-}$ PTEN$^{f/f}$ mice treated with Palbociclib, following the treatment schemes shown in Sup.Fig.6A and Sup.Fig.7A. Moreover, Ki-67 expression was also reduced in both tissues treated with the inhibitor (Sup.Fig.6D and Sup.Fig.7D), indicating that Palbociclib is effective at decreasing tumor cell proliferation both in thyroid and prostate. Surprisingly, histopathological analysis revealed that neither thyroid hyperplasias nor prostate neoplasias incidences were reduced by Palbociclib (Sup.Fig.6C and Sup.Fig.7C).

**Endometrial neoplasia response to Palbociclib correlates with Rb phosphorylation on Ser780 *in vivo*.**

We intended to investigate the underlying molecular mechanism explaining anti-tumoral effect of Palbociclib *in vivo* on endometrium. We analyzed by immunohistochemistry the expression of p-Rb (Ser780) in the tissues after short course and long-term treatment with the inhibitor.

The experimental workflow diagram for short-course treatment is showed in figure 3A. Palbociclib treatment led to a potent reduction of p-Rb (Ser780) in the endometrium, regardless of the dose tested (Fig.3B and Sup.Fig.8A). Surprisingly, the reduction of p-Rb (Ser780) levels was not observed in the endometrium after 21 days of treatment (Fig.3C and Sup.Fig.8B). In our hands, Palbociclib was not effective at reducing Rb phosphorylation neither in thyroid nor prostate (Fig.3B and 3C, Sup.Fig.8C and 8D).

It has been suggested that in the absence of Cyclin D-CDK4/6 activity, the phosphorylation of p-Rb could be carried out by Cyclin E-CDK2 in a scenario with low activity of CDK inhibitors such as p27[12,31,32]. After long treatment with Palbociclib in the endometrium, our results pointed out two different situations. On the one hand, some mice displayed high levels of p-ERK, and this increment was concomitant with high expression of Cyclin D1, Cyclin E, p27 and p-Rb. On the other hand, mice presenting lower levels of p-ERK showed less expression of Cyclin D1, Cyclin E, p27 and p-Rb. No significant changes were observed on p-AKT, p-S6K and CDK2 levels (Sup.Fig.8E). Even though the presence of Palbociclib abrogates the Cyclin D-CDK4/6 activity, these findings lead us to hypothesize that D-type Cyclins present in the cells still bind to CDK inhibitors, allowing Cyclin E-CDK2 complexes to phosphorylate p-Rb.

**Palbociclib treatment slows down endometrial tumor progression and increases overall mice survival.**

The therapeutical benefits of Palbociclib (administered for 21 days) on PTEN deficient endometrial carcinomas encouraged us to study the effects of chronic exposure to the inhibitor. The treatment scheme is shown in figure 4A. Chronic treatment with Palbociclib

induced a significant increase of mice survival. Cre:ER$^{T+/-}$ PTEN$^{fl/fl}$ treated females presented a median survival of 47 days, whereas this value was reduced to 32 days for the untreated ones (Fig.4B).

In endometrium, Palbociclib induced a delay in the development of EIN after PTEN loss. However, Palbociclib treated females finally displayed severe hyperplasia and EIN (Fig.4E). As depicted by figure 4C and 4D, macroscopic and histological analysis revealed no differences between PTEN deficient thyroids treated or not with the inhibitor. Collectively, these results suggest that Palbociclib treatment slows down tumor progression, allowing increased mice survival. Nevertheless, it does not cause a significant regression of endometrial and thyroid malignancies induced by PTEN loss.

**Palbociclib induces an anti-proliferative effect *in vitro* on human endometrial carcinoma cell lines.**

As it has been previously described, Palbociclib treatment reduces the proliferation of multiple human tumoral cell lines[33]. Having demonstrated the drug anti-tumoral effect in PTEN deficient endometrial carcinomas in mice, we aimed to determine its therapeutic potential in different human endometrial cancer models. We first monitored the viability of two EC cell lines, HEC-1A and MFE-296, after Palbociclib treatment by a MTT cytotoxicity assay. Both cell lines exposed to different concentrations of Palbociclib (2.5, 5 and 10 μM) for 48 hours presented a significant decrease in cell viability (Sup.Fig.9A). Next, we also observed that treatment of HEC-1A and MFE-296 cells with 5 μM and 10 μM Palbociclib for 48 hours resulted in a G1 phase arrest, preventing cells from entering S

phase (Sup.Fig.9B). Finally, as shown in supplementary figure 9C, Palbociclib also significantly reduced glandular size of HEC-1A cells when growing in three dimensions.

**Palbociclib exhibits anti-tumor activity against human endometrial cancer.**

Given that Palbociclib showed anti-proliferative effect on endometrial carcinoma cell lines *in vitro*, we aimed to assess whether the inhibitor presents anti-tumoral activity *in vivo*. Mice bearing HEC-1A or MFE-296 subcutaneous tumors were daily treated with Palbociclib at a dose of 150 mg/kg for 15 days by oral gavage. Interestingly, Palbociclib treatment led to a significant marked reduction in tumor growth (Fig.5A and 5C) with a concomitant decrease in Ki-67 expression (Fig.5B and 5D) when compared to vehicle treated animals. Taken together, these data indicate that Palbociclib inhibits tumoral growth of subcutaneously injected HEC-1A and MFE-296 cell lines into SCID mice.

In order to circumvent the limitations of conventional pre-clinical models in terms of translational research, we have also generated a patient-derived tumor xenograft model using a primary PTEN deficient endometrioid endometrial carcinoma (Fig.6A). Endometrial carcinoma sample was injected subcutaneously in female mice and the effects of Palbociclib were assessed for ten days. As depicted in figure 6B and 6C, Palbociclib impaired endometrial tumorigenesis by decreasing tumor growth in those mice treated with the drug. Furthermore, PDX treated with Palbociclib displayed a marked reduction of Ki-67 expression when compared with the untreated ones (Fig.6D). Finally, no significant reduction of p-Rb levels was observed after Palbociclib treatment (Fig.6E).

## Discussion

In the present work, we have investigated the role of Cyclin D-CDK4/6 axis in PTEN deficient endometrial tumors.

We have observed that endometrial carcinomas induced by PTEN loss show higher expression of Cyclin D1 than normal tissue, consistent with previous evidences[34]. However, the direct effect of PTEN on Cyclin D1 expression is controversial. For instance, it has been reported that the mutant PTEN-G129E form reduces Cyclin D1 levels in a breast cancer model[28]. Some endometrial carcinomas present some mutations in this lipid-phosphatase domain (G129D/E/R/V). It will be interesting to determine the effect of these PTEN mutant forms on Cyclin D1 levels. Nevertheless, our results are not comparable with the above mentioned, as we work with a model of PTEN loss. We have focused on PTEN deficient endometrial tumors, as they represent an important part of the total cases. Therefore, it seems that Cyclin D1 participates somehow in PTEN-driven endometrial malignancies, but the underlying mechanism has not been completely elucidated.

Here, we have evaluated the efficacy of Palbociclib in endometrial carcinomas in PTEN deficient mice. Our results pointed out that Palbociclib reduces tumor cell proliferation and disrupts the tumorigenic process in the endometrium. Interestingly, Cyclin D1 deficiency alone already decreases the extent of endometrial lesions.

Noteworthy, our results suggest that thyroid and prostate PTEN-deficient tumor maintenance exhibit dependence on Cyclin D-CDK4/6 axis, as Palbociclib decreases cell proliferation in both tissues. Consistently, Comstock and colleagues have reported anti-

proliferative effect of Palbociclib on prostate human tumor tissues *ex vivo*[35]. Surprisingly, neither prostate nor thyroid tumorigenesis is disrupted after Palbociclib administration in our mouse model. However, it has been reported a functional collaboration between p18 and PTEN in tumor suppression[36]. In this model, Cyclin D-CDK4/6 axis is exacerbated during development and before the appearance of tumors. In contrast, in our model, Palbociclib is given at the onset of malignancies. The distinct temporal intervention can lead to different response patterns. A raising question is why thyroid and prostate malignancies are dependent on Cyclin D-CDK4/6 inhibition for tumor maintenance but not for tumorigenesis. Such question can be explained because of Cyclin D-CDK4/6 axis proliferation-independent functions[37].

Therapeutic intervention on cell cycle has been proposed as an effective anti-tumor therapy[38,39]. Numerous clinical trials are ongoing to unveil the therapeutic benefit of Palbociclib both alone and in combinatorial approaches[38-40]. Patient-derived tumor xenografts represent an advanced pre-clinical model[41,42]. Here, we provide evidence that Palbociclib has therapeutic potential in a model of primary PTEN deficient endometrial carcinoma. However, Palbociclib has failed inducing tumor regression and cytotoxic effects. It is imperative to develop Palbociclib combinations with some cytotoxic agents. Some *in vitro* studies performed with breast cancer cell lines report antagonistic activity between Palbociclib and some chemotherapeutics[43,44]. Nevertheless, with proper cell cycle synchronization, synergistic killing effect is achieved in multiple models[45-47]. Noteworthy, Palbociclib is the first cell-cycle inhibitor that demonstrates broad-ranging efficacy in many tumor types. Therefore, it seems reasonable to consider Palbociclib combinations as a valuable promise[40].

Data from several groups have asserted that the status of p-Rb protein is critical for Palbociclib activity[33,35,38-40] and loss of Rb leads to drug resistance[38]. In our model, Palbociclib treatment only reduces p-Rb in the endometrium after acute treatment, but not in other tissues and longer treatments. Restoration of p-Rb levels may explain why Palbociclib fails to cause disease regression after long-term treatment in the endometrium. However, the role of Rb as a prognostic factor for Palbociclib treatment is still unclear. Consistent with this, we have found that PDX samples, which showed reduced proliferation and tumor growth after Palbociclib treatment, do not exhibit decreased expression of p-Rb protein. Furthermore, it has been described that some patients, who do not present benefit after Palbociclib treatment, show decreased p-Rb[38,44,48]. In these cases, the presence of intact Rb function does not predict CDK4/6 dependence.

During cell division, Cyclin D-CDK4/6 sequesters CDK inhibitors such as p27, liberating Cyclin E-CDK2 activity, which in turn, phosphorylates Rb. A similar reasoning could be used to explain the presence of p-Rb during Palbociclib treatment. However, after long treatment with Palbociclib, we have found out two possible scenarios. On the one hand, we have observed low levels of Cyclin D1, p27 and Cyclin E. On the other hand, after ERK activation, we have detected an up-regulation of the mentioned proteins, which correlates with an increment of p-Rb protein expression. We propose here that although Palbociclib inhibits Cyclin D-CDK4/6 kinase activity, Cyclin D1 still retains the ability to sequester p27 and relieve Cyclin E. In this way, Cyclin E expression may be enough to phosphorylate Rb protein when associated with CDK2[12,31,32]. Moreover, it is known that ERK pathway activation is necessary and sufficient to induce Cyclin D1 expression[49], so in the second context, the huge amount of Cyclin D1 may bypass Palbociclib inhibition and also

phosphorylate Rb protein. Furthermore, it would be interesting to determine the mechanism by which Cyclin E protein is up-regulated. Then, we hypothesize that Cyclin E may be responsible of Rb protein phosphorylation, during Palbociclib inhibition, as previously described[12]. Consistent with these findings, we have shown here that p-Rb expression is incremented in those mice expressing more Cyclin E.

Hitherto, we report the first pre-clinical study where the therapeutical potential of Palbociclib is evaluated in endometrial malignancies driven by PTEN deficiency. Our results highlight the Palbociclib clinical potential as an anti-cancer drug in the endometrium.

**Acknowledgments**

Supported by grants FIS PI13/00263, SAF2016-80157-R, PI13/01701, 2009SGR794, Grupos estables AECC (AECC2011), RETICS (RD12/0036/0013), Catalunya contra el cáncer, Programa de intensificación de la investigación, Instituto Carlos III and BFU 2013-42895-P. M.A.D. holds a predoctoral fellowship from Ministerio de Educación. We want to thank Mónica Domingo, Lidia Parra, Maria Carrelé and Anais Panosa for their technical support.

The authors declare no competing financial interests.

**Statement of author contributions**

Conceive experiments: MAD, CM, EG, XD and XMG

Carry out experiments: MAD, CM, RN, MS, EC and CMo

Analyze data: MAD, CM, NE, SG, JAS, ME, EG, XMG and XD

Write the paper: MAD, EG and XD

Generation of the figures: MAD, NE and IF

Approve the submitted and published versions: All authors

**Figure legends**

**Figure 1. Cyclin D1 deficiency displays a slight reduction of endometrial lesions.** A) Schematic diagram showing the experimental workflow. In short, mice were weaned 3 weeks after birth. At 8-10 weeks old, mice were injected with a single dose of tamoxifen to achieve PTEN ablation. Mice were sacrificed 4-6 weeks later. (B) Representative images showing HE staining (top panels) and immunostaining against Cyclin D1 (bottom panels) on uteri collected from Cre:$ER^{T-/-}$ $PTEN^{fl/fl}$ $CycD1^{-/-}$, Cre:$ER^{T+/-}$ $PTEN^{fl/fl}$ $CycD1^{+/+}$ and Cre:$ER^{T+/-}$ $PTEN^{fl/fl}$ $CycD1^{-/-}$ mice (10x), and evaluation of endometrial histology. No significant differences were observed by Chi square analysis. (C) Representative images and quantification of Ki-67 immunostaining. Data are from n=5 for each genotype and values are mean ± s.e.m. no significant differences were observed by t-test analysis. (D) Evaluation of Cyclin D1, Cyclin D2, CDK4, CDK6, CDK2 and Cyclin E expression by western blot in uteri collected from Cre:$ER^{T+/-}$ $PTEN^{fl/fl}$ $CycD1^{+/+}$ (WT) and Cre:$ER^{T+/-}$ $PTEN^{fl/fl}$ $CycD1^{-/-}$ (KO) mice. A representative image of n=3 biological replicates is shown for each genotype. Tubulin serves as loading control. Immunoreactive bands were quantified by densitometry analysis using ImageJ software. Relative levels values are expressed using tubulin as a reference. $**P < 0.01$, by t-test analysis. (E) Representative images of p-Rb (Ser780) immunostaining.

**Figure 2. Palbociclib treatment reduces endometrial carcinomas in PTEN deficient mice.** (A) Schematic representation of the protocol used for Palbociclib administration. Briefly, mice were given a single daily dose of 100 mg/kg of the drug for 21 consecutive

days, starting two weeks after PTEN deletion. (B) Representative images of HE staining (10x) and evaluation of uteri lesions from Palbociclib untreated and treated animals. ∗P < 0.05, by Chi square analysis. (C) Representative images and quantification of Ki-67 immunostaining performed on uterus dissected from mice treated or not with the drug. Data are from n=5 for each genotype and values are mean ± s.e.m. ∗∗P < 0.01, by t-test analysis.

**Figure 3. Tumor responses to Palbociclib in the endometrium correlate with Rb phosphorylation on Ser780 *in vivo.*** (A) Experimental workflow diagram showing the procedure used for Palbociclib acute treatment. Briefly, mice were treated with 75, 100 or 150 mg/kg of Palbociclib for three consecutive days, starting two weeks after PTEN deletion. (B) Representative images of p-Rb immunostaining performed on uteri (upper panel), thyroid (central panel) and prostate (bottom panel) dissected from mice after short curse of Palbociclib. (C) Representative images of p-Rb immunostaining performed on uteri (left), thyroid (central panel) and prostate (right) dissected from mice after 21 days of treatment with Palbociclib.

**Figure 4. Effects of Palbociclib chronic treatment in PTEN deficient endometrial carcinomas and thyroid hyperplasias.** (A) Schematic representation of the protocol used for Palbociclib administration. Briefly, mice were given a single daily dose of 100 mg/kg of the drug for 5 consecutive days followed by 2 days off treatment until mice required euthanasia, starting two weeks after PTEN deletion. (B) Kaplan-Meier survival curve. ∗∗∗P < 0.001, by Mantel-Cox test, followed by the Gehan-Breslow-Wilcoxon test. (C) Macroscopic images of thyroids from Palbociclib treated and untreated mice. (D) Representative images of HE staining (10x) and evaluation of thyroid lesions. No significant differences were observed by Chi square test. (E) Representative images of HE

staining (10x) and evaluation of uteri lesions from Palbociclib untreated and treated animals. No significant differences were observed by Chi square analysis.

**Figure 5. Palbociclib treatment reduces *in vivo* growth of endometrial carcinoma cell lines tumors.** SCID mice bearing HEC-1A or MFE-296 subcutaneous tumors were treated daily by oral gavage with 150 mg/kg Palbociclib for 15 days. (A and C) Comparison of representative vehicle and Palbociclib treated HEC-1A (A) or MFE-296 (C) xenograft tumors, and graph of tumor growth over time. ∗∗∗P < 0.001, by two-way ANOVA, followed by the Bonferroni post hoc comparison test. (B and D) Representative images and quantification of Ki-67 immunostaining performed on HEC-1A (B) or MFE-296 (D) subcutaneous tumors from mice treated or not with the drug. Data are from n=4 for each group and values are mean ± s.e.m. ∗∗P < 0.01, by t-test analysis.

**Figure 6. CDK4/6 inhibition by Palbociclib in a PTEN deficient PDX impairs endometrial carcinogenesis.** (A) Representative images of PTEN immunostaining performed on patient-derived endometrioid endometrial carcinoma. (B) Comparison of representative vehicle and Palbociclib treated PDX, and graph of tumor growth over time. ∗∗P < 0.01, by two-way ANOVA, followed by the Bonferroni post hoc comparison test. (C) Slope of tumor growth at day 8 and 10 of treatment. ∗∗P < 0.01, by t-test analysis. (D) Representative images and quantification of Ki-67 immunostaining performed on PDX treated or not with the drug. Data are from n=3 for each group and values are mean ± s.e.m. ∗∗∗P < 0.001, by t-test analysis. (E) Representative images of p-Rb immunostaining performed on PDX treated or not with Palbociclib.

**Supplementary figure legends**

**Supplementary Figure 1.** Breeding scheme for the mice used in this study.

**Supplementary Figure 2. PTEN deletion causes an increase of Cyclin D1 and Ki-67 expression.** Uteri, thyroids and prostates from Cre:$ER^{T-/-}$ $PTEN^{fl/fl}$ or Cre:$ER^{T+/-}$ $PTEN^{fl/fl}$ mice were analyzed 6-8 weeks after tamoxifen injection. (A, B and C). Representative images showing HE staining, Cyclin D1 immunohistochemistry and quantification on the endometrium (A), thyroid (B) and prostate (C) from Cre:$ER^{T-/-}$ $PTEN^{fl/fl}$ and Cre:$ER^{T+/-}$ $PTEN^{fl/fl}$ mice (10x). Data are from n=5 for each genotype and values are mean ± s.e.m. $*P < 0.05$ $**P < 0.01$, by t-test analysis (D) Evaluation of PTEN and Cyclin D1 expression by western blot in epithelial endometrial three-dimensional cultures. Tubulin serves as loading control. (E-F) Thyroid and prostate protein lysates were subjected to western blot analysis for Cyclin D1 expression. β-Actin serves as loading control. (G) Representative images showing Ki-67 immunohistochemistry on the endometrium (upper panel), thyroid (central panel) and prostate (bottom panel) from Cre:$ER^{T-/-}$ $PTEN^{fl/fl}$ and Cre:$ER^{T+/-}$ $PTEN^{fl/fl}$ mice (10x).

**Supplementary Figure 3. Cyclin D1 is dispensable for PTEN driven thyroid hyperplasias.** (A) Schematic diagram showing the experimental workflow. (B) Comparison of representative wild-type and $CycD1^{-/-}$ thyroids 4-6 weeks after PTEN deletion. (C) Representative images showing HE staining (top panels) and immunostaining against Cyclin D1 (bottom panels) on thyroids collected from Cre:$ER^{T-/-}$ $PTEN^{fl/fl}$ $CycD1^{-/-}$, Cre:$ER^{T+/-}$ $PTEN^{fl/fl}$ $CycD1^{+/+}$ and Cre:$ER^{T+/-}$ $PTEN^{fl/fl}$ $CycD1^{-/-}$ mice (10x), and evaluation of thyroid histology. No significant differences were observed by Chi square analysis. (D) Representative images and quantification of Ki-67 immunostaining. Data are from n=5 for

each genotype and values are mean ± s.e.m. no significant differences were observed by t-test analysis. (E) Evaluation of Cyclin D1, Cyclin D2, CDK4, CDK6, CDK2 and Cyclin E expression by western blot in thyroids collected from Cre:ER$^{T+/-}$ PTEN$^{fl/fl}$ CycD1$^{+/+}$ (WT) and Cre:ER$^{T+/-}$ PTEN$^{fl/fl}$ CycD1$^{-/-}$ (KO) mice. A representative image of n=3 biological replicates is shown for each genotype. Tubulin serves as loading control. Immunoreactive bands were quantified by densitometry analysis using ImageJ software. Relative levels values are expressed using tubulin as a reference. $**P < 0.01$, by t-test analysis. (F) Representative images of p-Rb (Ser780) immunostaining.

**Supplementary Figure 4. Cyclin D1 is dispensable for PTEN driven prostatic neoplasias.** (A) Schematic diagram showing the experimental workflow. (B) Comparison of wild-type and CycD1$^{-/-}$ prostates 4-6 weeks after PTEN deletion. (C) Representative images showing HE staining (top panels) and immunostaining against Cyclin D1 (bottom panels) on prostates collected from Cre:ER$^{T-/-}$ PTEN$^{fl/fl}$ CycD1$^{-/-}$, Cre:ER$^{T+/-}$ PTEN$^{fl/fl}$ CycD1$^{+/+}$ and Cre:ER$^{T+/-}$ PTEN$^{fl/fl}$ CycD1$^{-/-}$ mice (10x), and evaluation of prostate histology. No significant differences were observed by Chi square analysis. hgPIN means high-grade PIN. (D) Representative images and quantification of Ki-67 immunostaining. Data are from n=5 for each genotype and values are mean ± s.e.m. no significant differences were observed by t-test analysis. (E) Evaluation of Cyclin D1, Cyclin D2, CDK4, CDK6, CDK2 and Cyclin E expression by western blot in prostates collected from Cre:ER$^{T+/-}$ PTEN$^{fl/fl}$ CycD1$^{+/+}$ (WT) and Cre:ER$^{T+/-}$ PTEN$^{fl/fl}$ CycD1$^{-/-}$ (KO) mice. A representative image of n=3 biological replicates is shown for each genotype. Tubulin serves as loading control. Immunoreactive bands were quantified by densitometry analysis

using ImageJ software. Relative levels values are expressed using tubulin as a reference. ∗P < 0.05, by t-test analysis. (F) Representative images of p-Rb (Ser780) immunostaining.

**Supplementary Figure 5. Cyclin D-CDK4/6 axis inhibition by Palbociclib induces a decrease of cell proliferation *in vitro*.** (A) RT-qPCR analysis of Cyclin D1, Cyclin D2 and Cyclin D3 mRNA expression from epithelial endometrial 3D cultures. Data are from n=4 experimental replicates (independent mRNA preparations) and values are mean ± s.e.m. ∗P < 0.05, by t-test analysis. (B) Representative phase contrast images and measurement of glandular diameter of endometrial epithelial 3D cultures from Cre:$ER^{T+/-}$ $PTEN^{f/f}$ exposed (PTEN KO) or not (PTEN WT) to tamoxifen to induce PTEN deletion, and treated or not with Palbociclib (5 μM) for 48 hours. Three independent experiments were performed. Error bars represent mean ± s.e.m. ∗P < 0.05 ∗∗P < 0.01, by t-test analysis. Scale bars: 100 μm. (C) Upper, images showing representative staining of BrdU positive cells from endometrial epithelial 3D cultures treated (PTEN KO) or not (PTEN WT) with tamoxifen to induce PTEN deletion and in combination or not with Palbociclib at 2.5, 5 and 10 μM doses. Bottom, quantification of the number of BrdU positive cells from the same cultures. Nuclei were evidenced by Hoechst staining. Scale bar: 50 μm. Data are from n=3 experimental replicates and values are mean ± s.e.m. ∗P < 0.05 ∗∗P < 0.01∗∗∗ P < 0.001, by t-test analysis.

**Supplementary Figure 6. Palbociclib effects on PTEN deficient thyroid hyperplasias.** (A) Schematic representation of the protocol used for Palbociclib administration. (B) Macroscopic images and weight of thyroids from Palbociclib treated mice. ∗∗∗P< 0.001, by t-test analysis. (C) Representative images of HE staining (10x) and evaluation of thyroid lesions. No significant differences were observed by Chi square analysis. (D)

Representative images and quantification of Ki-67 immunostaining performed on thyroids dissected from mice treated or not with Palbociclib. Data are from n=5 for each genotype and values are mean ± s.e.m. ∗P < 0.05, by t-test analysis.

**Supplementary Figure 7. Palbociclib effects on PTEN deficient prostate neoplasias.** (A) Schematic representation of the protocol used for Palbociclib administration. (B) Macroscopic images and weight of prostates from Palbociclib treated mice. ∗∗∗P< 0.001, by t-test analysis. (C) Representative images of HE staining (10x) and evaluation of prostate lesions. No significant differences were observed by Chi square analysis. hgPIN means high-grade PIN. (D) Representative images and quantification of Ki-67 immunostaining performed on prostates dissected from mice treated or not with Palbociclib. Data are from n=5 for each genotype and values are mean ± s.e.m. ∗∗P < 0.01, by t-test analysis.

**Supplementary Figure 8. p-Rb IHC Quantification and western blot analysis.** (A) Quantification, by automated ACIS III system, of p-Rb IHC performed on endometrium after short-course treatment with Palbociclib. Data are from n=3 for each group and values are mean ± s.e.m. ∗∗P < 0.01, by t-test analysis. (B,C and D) IHC quantification results of p-Rb (Ser780) on endometrium (B), thyroid (C) and prostate (D) dissected from animals Cre:$ER^{T+/-}$ $PTEN^{f/f}$ treated with vehicle or Palbociclib for 21 consecutive days. Data are from n=6 for each group and values are mean ± s.e.m. no significant differences were observed by t-test analysis. (E) Evaluation of p-S6K, p-AKT, Total AKT, p-ERK, pan-ERK, Cyclin D1, CDK2, Cyclin E, p27 and p-Rb expression by western blot in uterus collected from Cre:$ER^{T+/-}$ $PTEN^{fl/fl}$ treated with Palbociclib for 21 days. n=5 biological replicates is shown. Tubulin serves as loading control.

**Supplementary Figure 9. Palbociclib treatment exhibits an anti-proliferative effect *in vitro* on human endometrial carcinoma cell lines.** (A) HEC-1A and MFE-296 cells were treated with 2.5, 5 and 10 μM Palbociclib for 48h and cell viability was evaluated by MTT. Three independent experiments were performed. Results are expressed as percentage of survival over control values. $*P < 0.05$ $**P < 0.01$ $***P < 0.001$, by two-way ANOVA, followed by the Bonferroni post hoc comparison test. (B) After 48 hours treatment of HEC-1A and MFE-296 endometrial carcinoma cell lines with 5 μM and 10 μM Palbociclib, propidium iodide staining was performed to evaluate DNA content by flow cytometry. Data are from n=3 experimental replicates. $**P < 0.01$ $***P < 0.001$, by one-way ANOVA, followed by the Tukey's multiple comparison test. (C) HEC-1A three-dimensional cultures were treated for 48 hours with 5 μM and 10 μM Palbociclib and spheroid diameter was evaluated. Three independent experiments were performed. $***P < 0.001$, by one-way ANOVA, followed by the Tukey's multiple comparison test.

## References


1. Maehama T, Dixon JE. The tumor suppressor, PTEN/MMAC1, dephosphorylates the lipid second messenger, phosphatidylinositol 3,4,5-trisphosphate. *J Biol Chem* 1998; **273**: 13375-13378.
2. Myers MP, Tonks NK. PTEN: sometimes taking it off can be better than putting it on. *Am J Hum Genet* 1997; **61**: 1234-1238.
3. Hollander MC, Blumenthal GM, Dennis PA. PTEN loss in the continuum of common cancers, rare syndromes and mouse models. *Nat Rev Cancer* 2011; **11**: 289-301.
4. Amant F, Moerman P, Neven P*, et al.* Endometrial cancer. *Lancet* 2005; **366**: 491-505.
5. Kandoth C, Schultz N, Cherniack AD*, et al.* Integrated genomic characterization of endometrial carcinoma. *Nature* 2013; **497**: 67-73.
6. Suzuki A, de la Pompa JL, Stambolic V*, et al.* High cancer susceptibility and embryonic lethality associated with mutation of the PTEN tumor suppressor gene in mice. *Curr Biol* 1998; **8**: 1169-1178.
7. Di Cristofano A, Pesce B, Cordon-Cardo C*, et al.* Pten is essential for embryonic development and tumour suppression. *Nat Genet* 1998; **19**: 348-355.
8. Podsypanina K, Ellenson LH, Nemes A*, et al.* Mutation of Pten/Mmac1 in mice causes neoplasia in multiple organ systems. *Proc Natl Acad Sci U S A* 1999; **96**: 1563-1568.
9. Mirantes C, Eritja N, Dosil MA*, et al.* An inducible knockout mouse to model the cell-autonomous role of PTEN in initiating endometrial, prostate and thyroid neoplasias. *Dis Model Mech* 2013; **6**: 710-720.
10. Casimiro MC, Velasco-Velázquez M, Aguirre-Alvarado C*, et al.* Overview of cyclins D1 function in cancer and the CDK inhibitor landscape: past and present. *Expert Opin Investig Drugs* 2014; **23**: 295-304.
11. Pestell RG. New roles of cyclin D1. *Am J Pathol* 2013; **183**: 3-9.
12. Barrière C, Santamaría D, Cerqueira A*, et al.* Mice thrive without Cdk4 and Cdk2. *Mol Oncol* 2007; **1**: 72-83.
13. Malumbres M, Barbacid M. Cell cycle, CDKs and cancer: a changing paradigm. *Nat Rev Cancer* 2009; **9**: 153-166.
14. Bartkova J, Lukas J, Strauss M*, et al.* Cyclin D1 oncoprotein aberrantly accumulates in malignancies of diverse histogenesis. *Oncogene* 1995; **10**: 775-778.
15. Cheung TH, Yu MM, Lo KW*, et al.* Alteration of cyclin D1 and CDK4 gene in carcinoma of uterine cervix. *Cancer Lett* 2001; **166**: 199-206.
16. Dickson C, Fantl V, Gillett C*, et al.* Amplification of chromosome band 11q13 and a role for cyclin D1 in human breast cancer. *Cancer Lett* 1995; **90**: 43-50.
17. Santamaria D, Ortega S. Cyclins and CDKS in development and cancer: lessons from genetically modified mice. *Front Biosci* 2006; **11**: 1164-1188.
18. Malumbres M, Barbacid M. Cell cycle kinases in cancer. *Curr Opin Genet Dev* 2007; **17**: 60-65.
19. Malumbres M, Pevarello P, Barbacid M*, et al.* CDK inhibitors in cancer therapy: what is next? *Trends Pharmacol Sci* 2008; **29**: 16-21.
20. Gohil K. Pharmaceutical Approval Update. *P T* 2015; **40**: 726-774.
21. Eritja N, Domingo M, Dosil MA*, et al.* Combinatorial therapy using dovitinib and ICI182.780 (fulvestrant) blocks tumoral activity of endometrial cancer cells. *Mol Cancer Ther* 2014; **13**: 776-787.

22. Eritja N, Chen BJ, Rodríguez-Barrueco R*, et al.* Autophagy orchestrates adaptive responses to targeted therapy in endometrial cancer. *Autophagy* 2017: 1-17.
23. Mirantes C, Dosil MA, Eritja N*, et al.* Effects of the multikinase inhibitors Sorafenib and Regorafenib in PTEN deficient neoplasias. *Eur J Cancer* 2016; **63**: 74-87.
24. Eritja N, Llobet D, Domingo M*, et al.* A novel three-dimensional culture system of polarized epithelial cells to study endometrial carcinogenesis. *Am J Pathol* 2010; **176**: 2722-2731.
25. Eritja N, Mirantes C, Llobet D*, et al.* Long-term estradiol exposure is a direct mitogen for insulin/EGF-primed endometrial cells and drives PTEN loss-induced hyperplasic growth. *Am J Pathol* 2013; **183**: 277-287.
26. Radu A, Neubauer V, Akagi T*, et al.* PTEN induces cell cycle arrest by decreasing the level and nuclear localization of cyclin D1. *Mol Cell Biol* 2003; **23**: 6139-6149.
27. Paramio JM, Navarro M, Segrelles C*, et al.* PTEN tumour suppressor is linked to the cell cycle control through the retinoblastoma protein. *Oncogene* 1999; **18**: 7462-7468.
28. Weng LP, Brown JL, Eng C. PTEN coordinates G(1) arrest by down-regulating cyclin D1 via its protein phosphatase activity and up-regulating p27 via its lipid phosphatase activity in a breast cancer model. *Hum Mol Genet* 2001; **10**: 599-604.
29. Fantl V, Stamp G, Andrews A*, et al.* Mice lacking cyclin D1 are small and show defects in eye and mammary gland development. *Genes Dev* 1995; **9**: 2364-2372.
30. Sicinski P, Donaher JL, Parker SB*, et al.* Cyclin D1 provides a link between development and oncogenesis in the retina and breast. *Cell* 1995; **82**: 621-630.
31. Geng Y, Yu Q, Sicinska E*, et al.* Deletion of the p27Kip1 gene restores normal development in cyclin D1-deficient mice. *Proc Natl Acad Sci U S A* 2001; **98**: 194-199.
32. Kozar K, Ciemerych MA, Rebel VI*, et al.* Mouse development and cell proliferation in the absence of D-cyclins. *Cell* 2004; **118**: 477-491.
33. Fry DW, Harvey PJ, Keller PR*, et al.* Specific inhibition of cyclin-dependent kinase 4/6 by PD 0332991 and associated antitumor activity in human tumor xenografts. *Mol Cancer Ther* 2004; **3**: 1427-1438.
34. Mirantes C, Dosil MA, Hills D*, et al.* Deletion of Pten in CD45-expressing cells leads to development of T-cell lymphoblastic lymphoma but not myeloid malignancies. *Blood* 2016; **127**: 1907-1911.
35. Comstock CE, Augello MA, Goodwin JF*, et al.* Targeting cell cycle and hormone receptor pathways in cancer. *Oncogene* 2013; **32**: 5481-5491.
36. Bai F, Pei XH, Pandolfi PP*, et al.* p18 Ink4c and Pten constrain a positive regulatory loop between cell growth and cell cycle control. *Mol Cell Biol* 2006; **26**: 4564-4576.
37. Hydbring P, Malumbres M, Sicinski P. Non-canonical functions of cell cycle cyclins and cyclin-dependent kinases. *Nat Rev Mol Cell Biol* 2016; **17**: 280-292.
38. Asghar U, Witkiewicz AK, Turner NC*, et al.* The history and future of targeting cyclin-dependent kinases in cancer therapy. *Nat Rev Drug Discov* 2015; **14**: 130-146.
39. Sherr CJ, Beach D, Shapiro GI. Targeting CDK4 and CDK6: From Discovery to Therapy. *Cancer Discov* 2016; **6**: 353-367.
40. Clark AS, Karasic TB, DeMichele A*, et al.* Palbociclib (PD0332991)-a Selective and Potent Cyclin-Dependent Kinase Inhibitor: A Review of Pharmacodynamics and Clinical Development. *JAMA Oncol* 2016; **2**: 253-260.
41. Hidalgo M, Amant F, Biankin AV*, et al.* Patient-derived xenograft models: an emerging platform for translational cancer research. *Cancer Discov* 2014; **4**: 998-1013.
42. Malaney P, Nicosia SV, Davé V. One mouse, one patient paradigm: New avatars of personalized cancer therapy. *Cancer Lett* 2014; **344**: 1-12.

43. McClendon AK, Dean JL, Rivadeneira DB*, et al.* CDK4/6 inhibition antagonizes the cytotoxic response to anthracycline therapy. *Cell Cycle* 2012; **11**: 2747-2755.
44. Roberts PJ, Bisi JE, Strum JC*, et al.* Multiple roles of cyclin-dependent kinase 4/6 inhibitors in cancer therapy. *J Natl Cancer Inst* 2012; **104**: 476-487.
45. Dean JL, McClendon AK, Knudsen ES. Modification of the DNA damage response by therapeutic CDK4/6 inhibition. *J Biol Chem* 2012; **287**: 29075-29087.
46. Menu E, Garcia J, Huang X*, et al.* A novel therapeutic combination using PD 0332991 and bortezomib: study in the 5T33MM myeloma model. *Cancer Res* 2008; **68**: 5519-5523.
47. Baughn LB, Di Liberto M, Wu K*, et al.* A novel orally active small molecule potently induces G1 arrest in primary myeloma cells and prevents tumor growth by specific inhibition of cyclin-dependent kinase 4/6. *Cancer Res* 2006; **66**: 7661-7667.
48. Leonard JP, LaCasce AS, Smith MR*, et al.* Selective CDK4/6 inhibition with tumor responses by PD0332991 in patients with mantle cell lymphoma. *Blood* 2012; **119**: 4597-4607.
49. Meloche S, Pouysségur J. The ERK1/2 mitogen-activated protein kinase pathway as a master regulator of the G1- to S-phase transition. *Oncogene* 2007; **26**: 3227-3239.

**A**

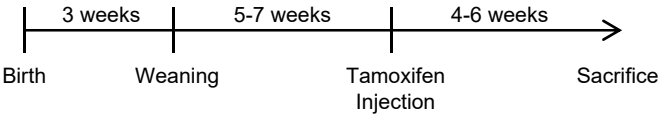


**B**

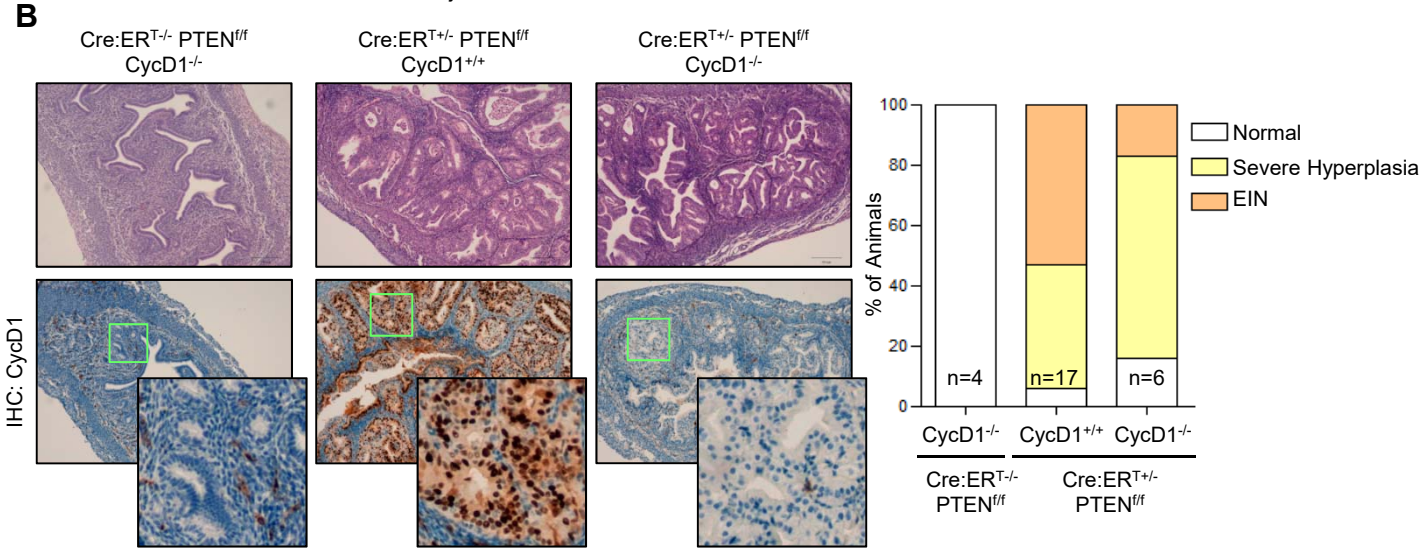


**C**

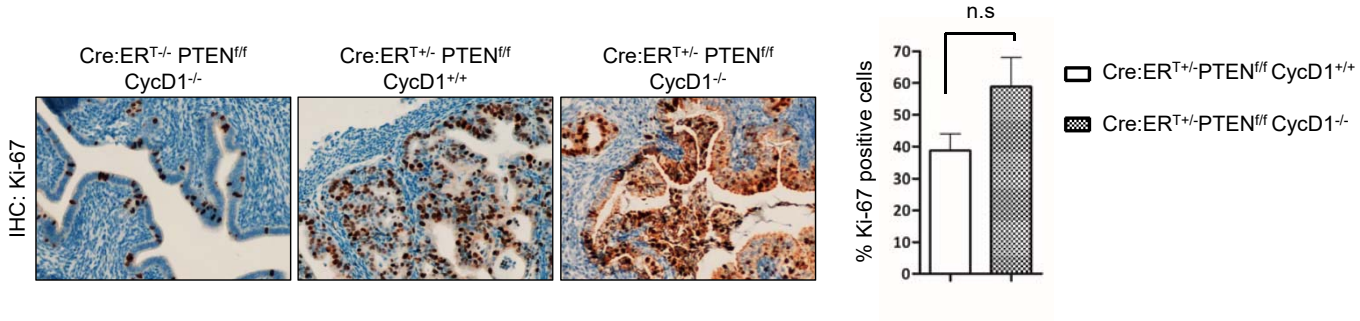


**D**

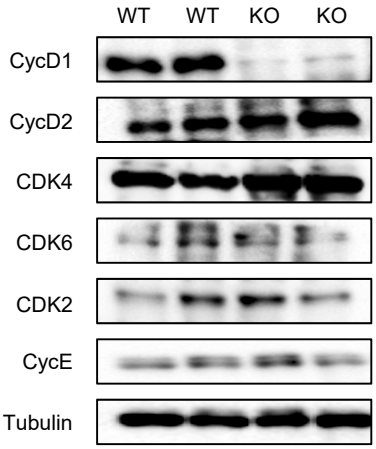


| | WT | KO | *p-value* |
|---|---|---|---|
| Relative fold increase of CycD1 Desvest | 1.031 ± 0.043 | 0.117 ± 0.077 | ***p=0.01* |
| Relative fold increase of CycD2 Desvest | 1.232 ± 0.329 | 1.772 ± 0.183 | *p=0.21* |
| Relative fold increase of CDK4 Desvest | 0.854 ± 0.207 | 1.433 ± 0.059 | *p=0.14* |
| Relative fold increase of CDK6 Desvest | 1.939 ± 1.329 | 1.826 ± 0.531 | *p=0.93* |
| Relative fold increase of CDK2 Desvest | 1,656 ± 0.928 | 1.613 ± 0.978 | *p=0.97* |
| Relative fold increase of CycE Desvest | 1.150 ± 0.213 | 1.268 ± 0.550 | *p=0.82* |

**E**

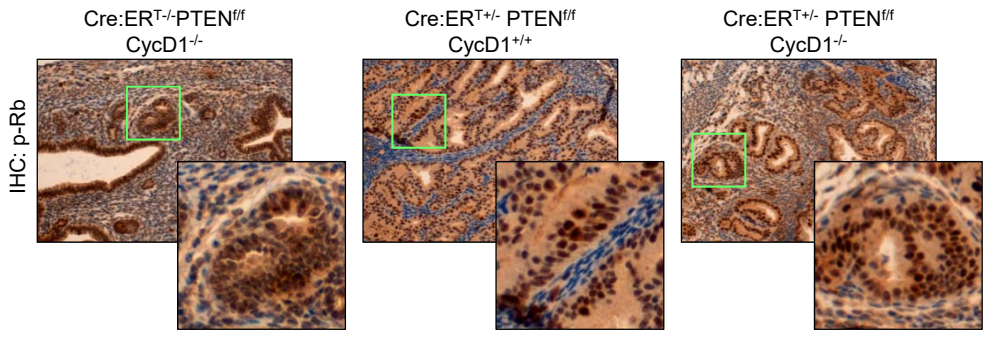

**A**

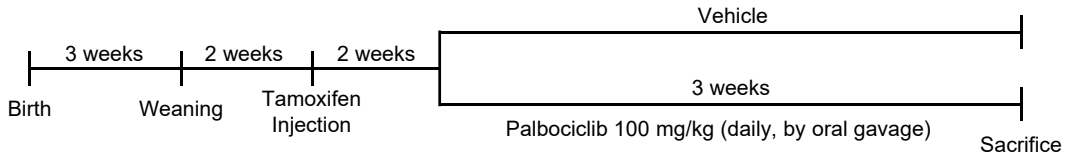
Vehicle
3 weeks
2 weeks
2 weeks
3 weeks
Birth
Weaning
Tamoxifen Injection
Palbociclib 100 mg/kg (daily, by oral gavage)
Sacrifice

**B**

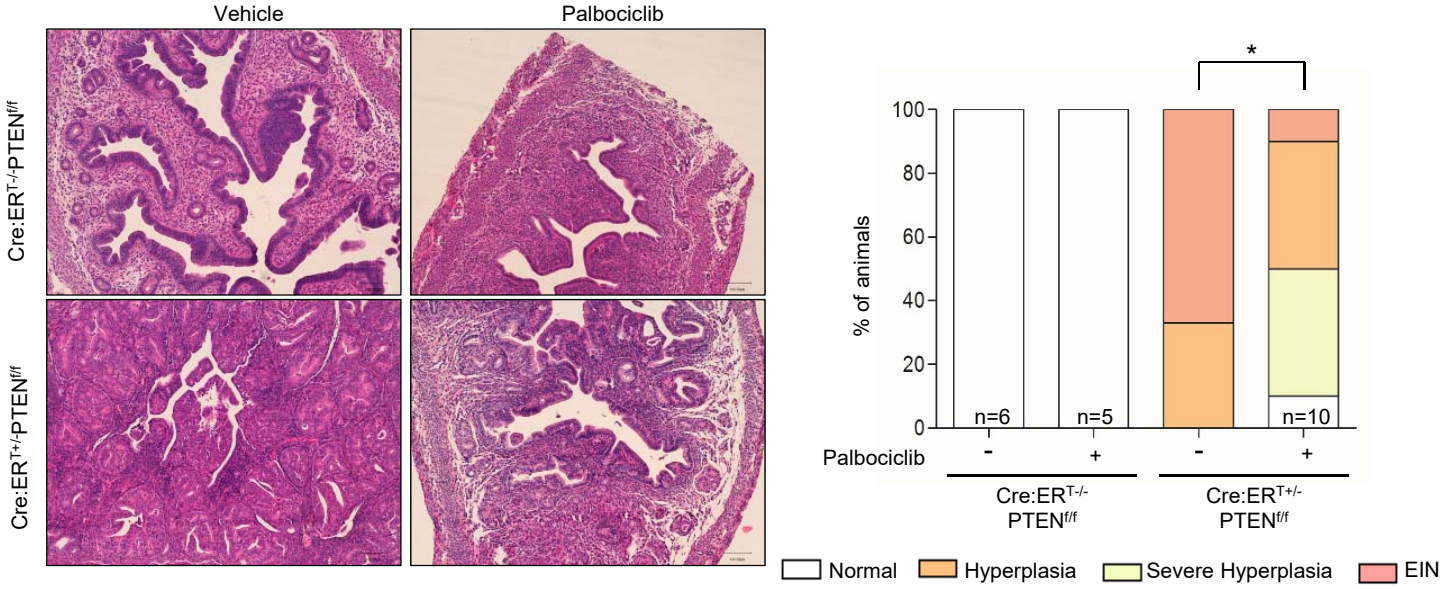
Vehicle
Palbociclib
Cre:ERT-/-PTENf/f
Cre:ERT+/-PTENf/f
% of animals
100
80
60
40
20
0
n=6
n=5
n=10
*
Palbociclib
-
+
-
+
Cre:ERT-/- PTENf/f
Cre:ERT+/- PTENf/f
Normal
Hyperplasia
Severe Hyperplasia
EIN

**C**

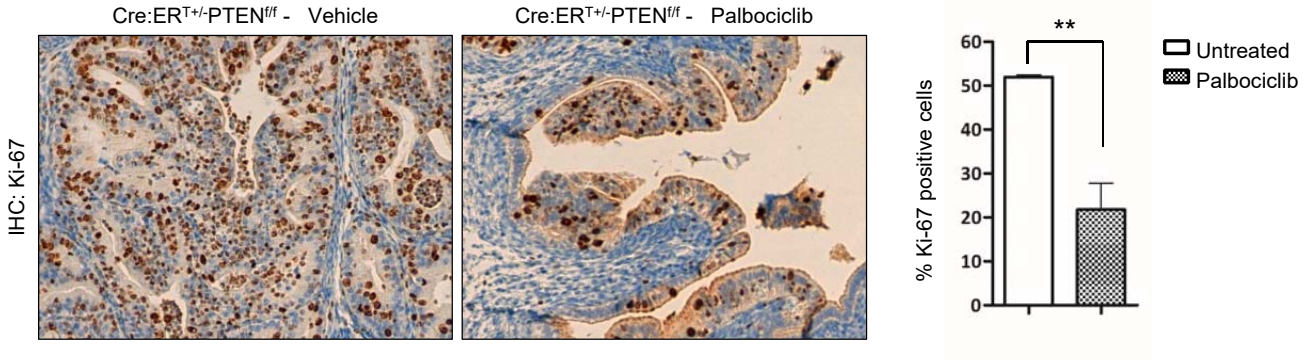
Cre:ERT+/-PTENf/f - Vehicle
Cre:ERT+/-PTENf/f - Palbociclib
IHC: Ki-67
% Ki-67 positive cells
60
50
40
30
20
10
0
**
Untreated
Palbociclib

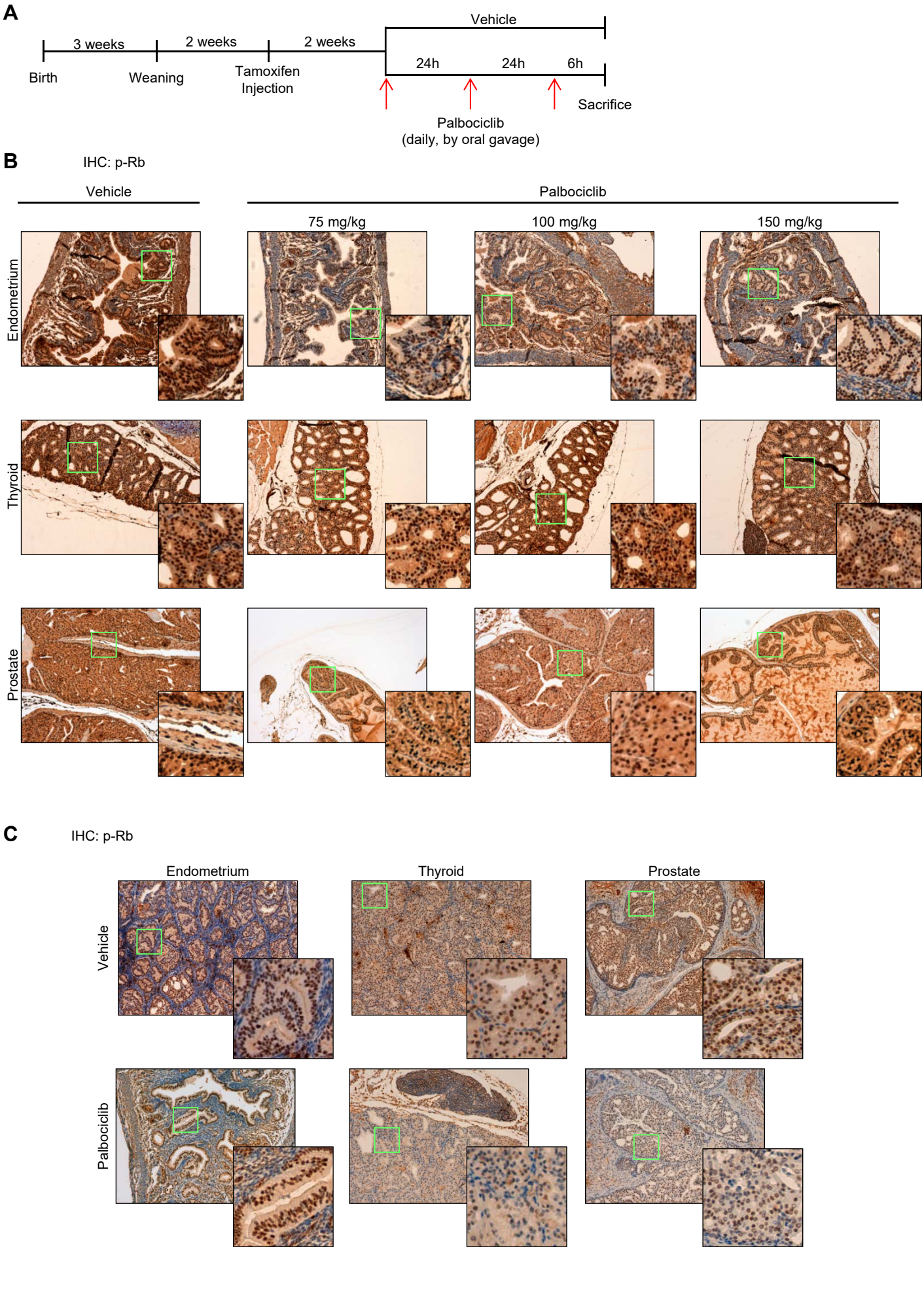
A
3 weeks
2 weeks
2 weeks
Vehicle
24h
24h
6h
Birth
Weaning
Tamoxifen Injection
Sacrifice
Palbociclib (daily, by oral gavage)
B
IHC: p-Rb
Vehicle
Palbociclib
75 mg/kg
100 mg/kg
150 mg/kg
Endometrium
Thyroid
Prostate
C
IHC: p-Rb
Endometrium
Thyroid
Prostate
Vehicle
Palbociclib

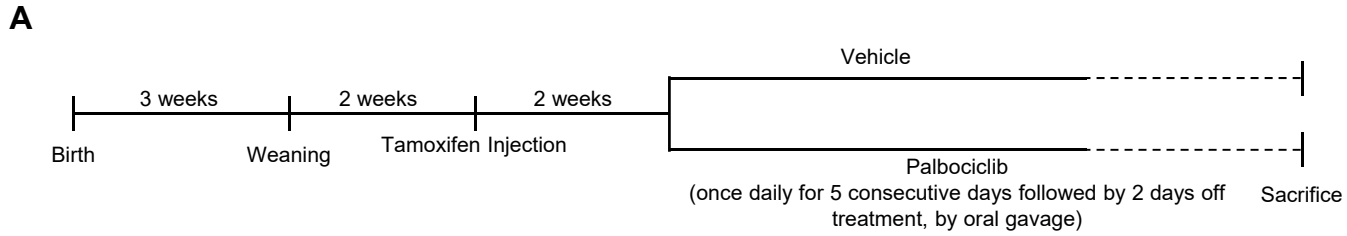
A
Vehicle
3 weeks
2 weeks
2 weeks
Birth
Weaning
Tamoxifen Injection
Palbociclib
(once daily for 5 consecutive days followed by 2 days off treatment, by oral gavage)
Sacrifice

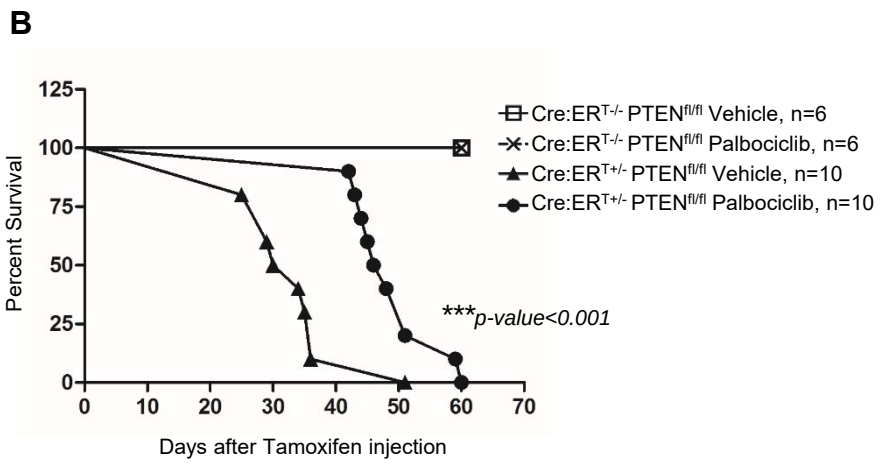
B
Percent Survival
125
100
75
50
25
0
0 10 20 30 40 50 60 70
Days after Tamoxifen injection
Cre:ERT-/- PTENfl/fl Vehicle, n=6
Cre:ERT-/- PTENfl/fl Palbociclib, n=6
Cre:ERT+/- PTENfl/fl Vehicle, n=10
Cre:ERT+/- PTENfl/fl Palbociclib, n=10
***p-value<0.001

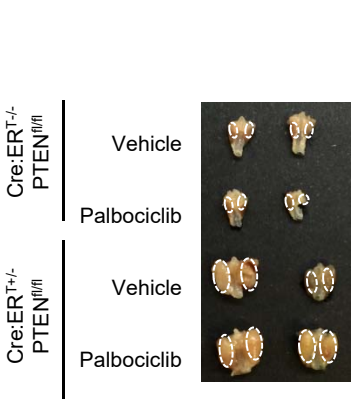
C
Cre:ERT-/- PTENfl/fl
Vehicle
Palbociclib
Cre:ERT+/- PTENfl/fl
Vehicle
Palbociclib

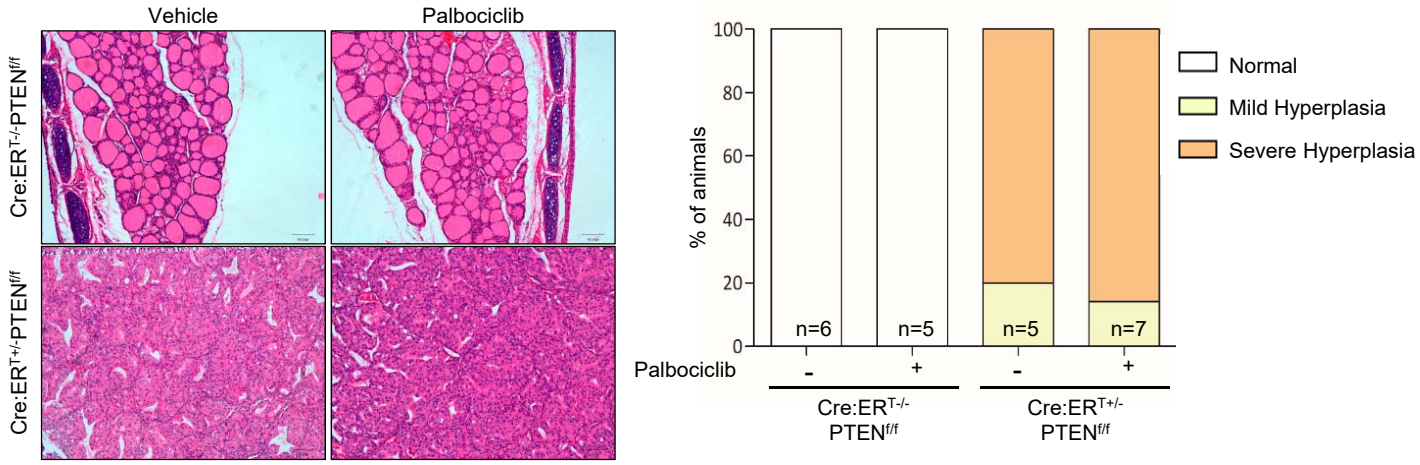
D
Vehicle
Palbociclib
Cre:ERT-/-PTENf/f
Cre:ERT+/-PTENf/f
% of animals
100
80
60
40
20
0
n=6
n=5
n=5
n=7
Palbociclib
-
+
-
+
Cre:ERT-/- PTENf/f
Cre:ERT+/- PTENf/f
Normal
Mild Hyperplasia
Severe Hyperplasia

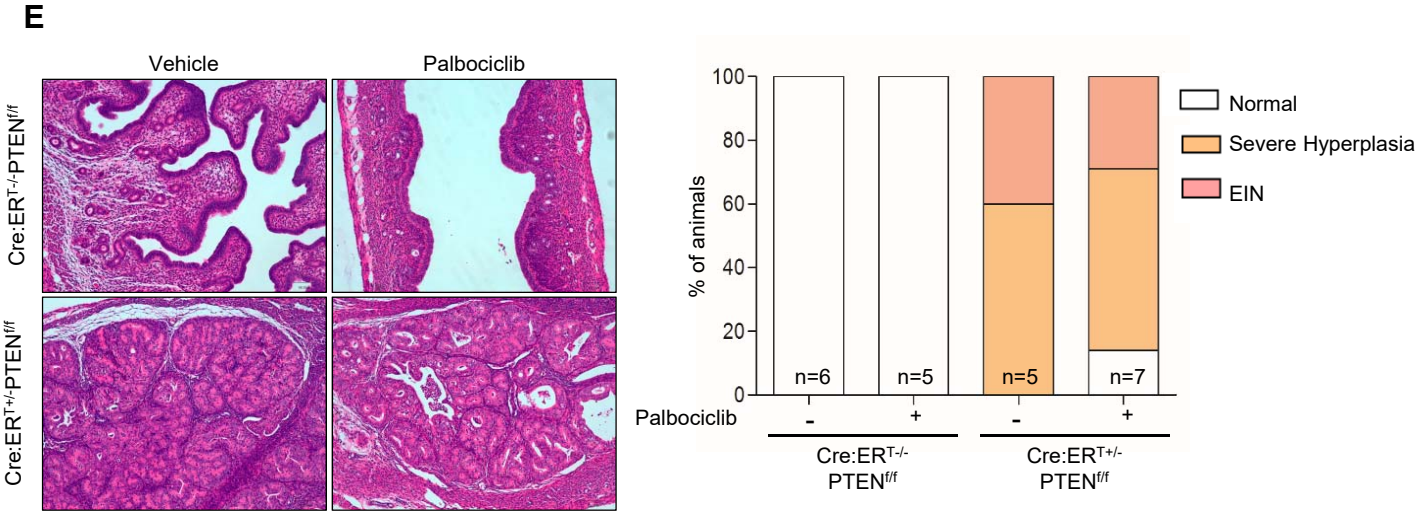
E
Vehicle
Palbociclib
Cre:ERT-/-PTENf/f
Cre:ERT+/-PTENf/f
% of animals
100
80
60
40
20
0
n=6
n=5
n=5
n=7
Palbociclib
-
+
-
+
Cre:ERT-/- PTENf/f
Cre:ERT+/- PTENf/f
Normal
Severe Hyperplasia
EIN

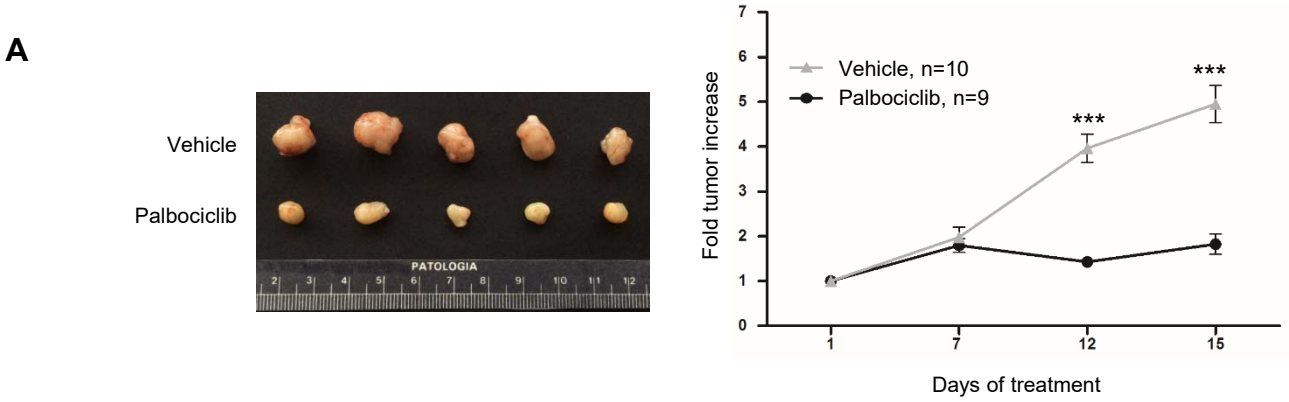
A
Vehicle
Palbociclib
PATOLOGIA
Vehicle, n=10
Palbociclib, n=9
***
***
Fold tumor increase
Days of treatment

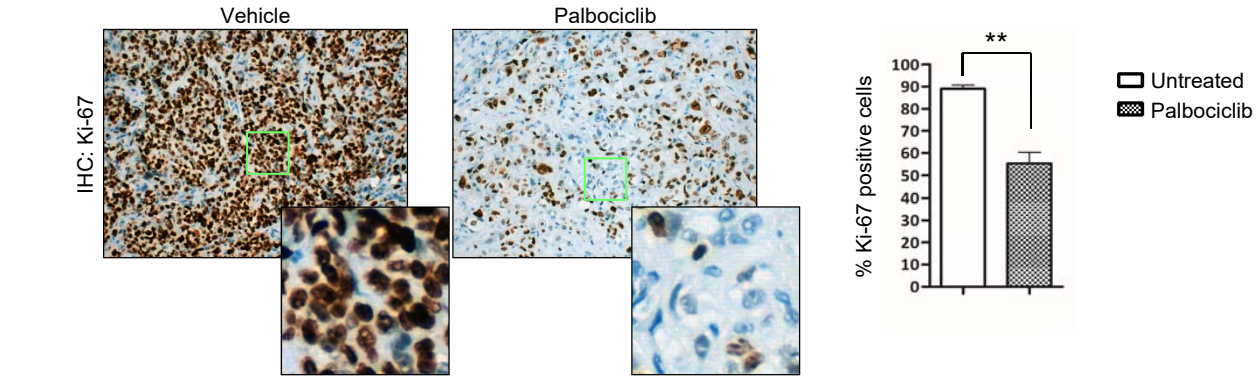
B
Vehicle
Palbociclib
IHC: Ki-67
**
% Ki-67 positive cells
Untreated
Palbociclib

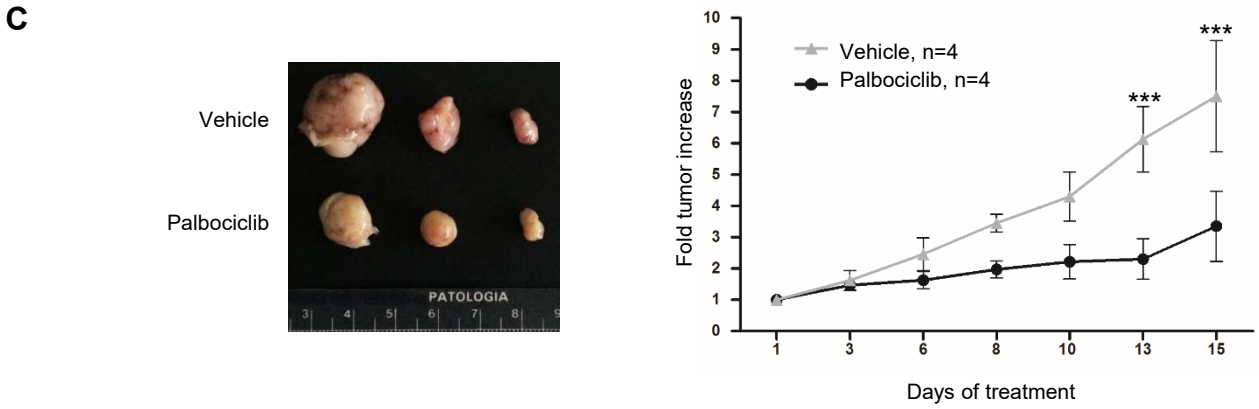
C
Vehicle
Palbociclib
PATOLOGIA
Vehicle, n=4
Palbociclib, n=4
***
***
Fold tumor increase
Days of treatment

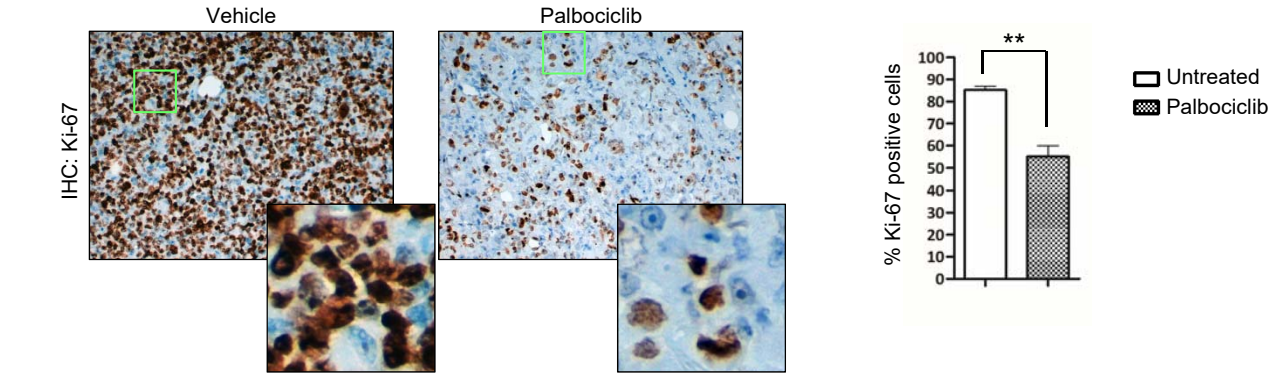
D
Vehicle
Palbociclib
IHC: Ki-67
**
% Ki-67 positive cells
Untreated
Palbociclib

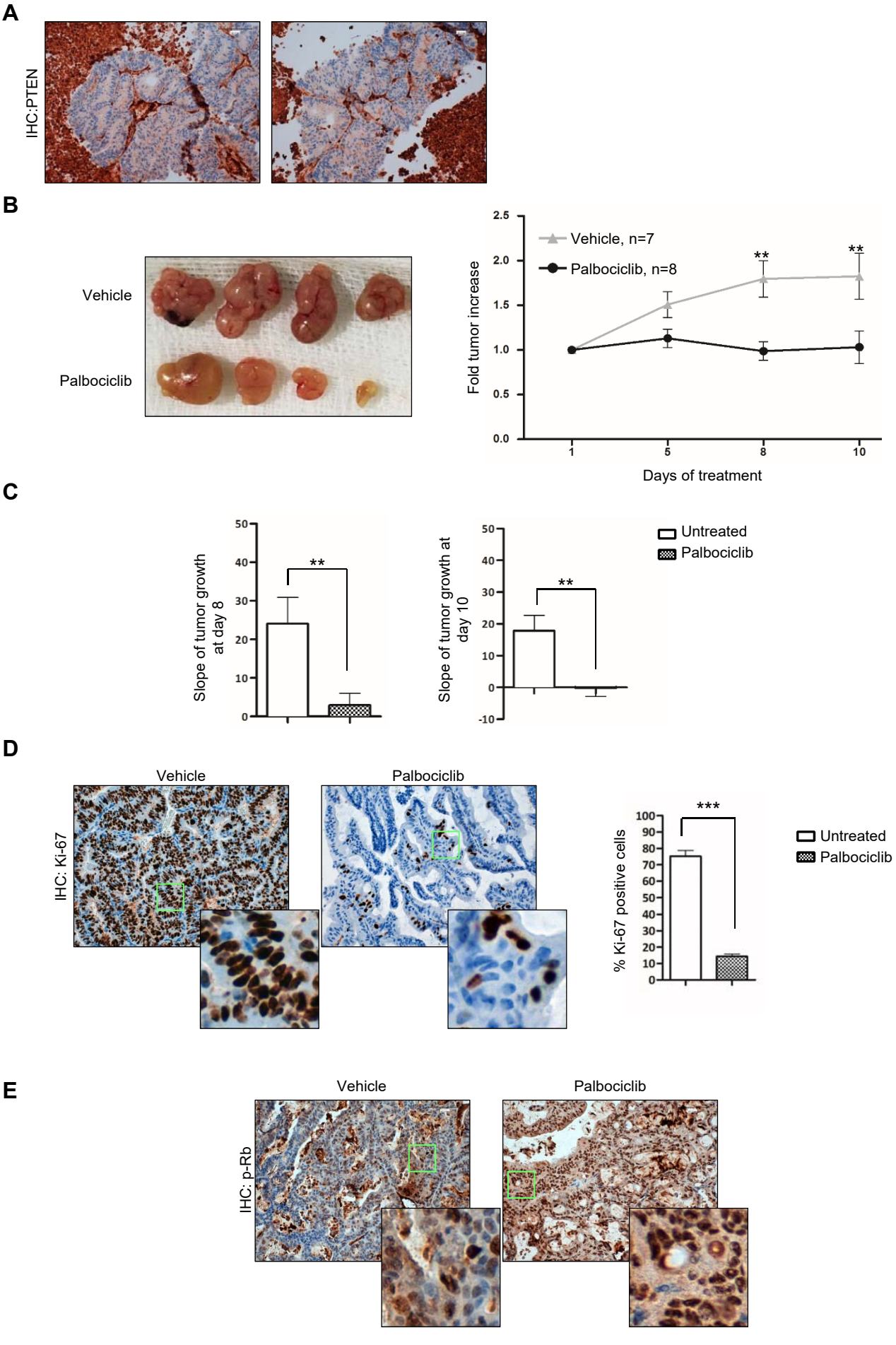
A
IHC:PTEN
B
Vehicle
Palbociclib
Vehicle, n=7
Palbociclib, n=8
Fold tumor increase
Days of treatment
C
Slope of tumor growth at day 8
Slope of tumor growth at day 10
Untreated
Palbociclib
D
Vehicle
Palbociclib
IHC: Ki-67
% Ki-67 positive cells
Untreated
Palbociclib
E
Vehicle
Palbociclib
IHC: p-Rb